

Lawrence Berkeley National Laboratory

Recent Work

Title

REACTIONS and WETTING BEHAVIOR IN THE ALUMINUM-FUSED SILICA SYSTEM

Permalink

<https://escholarship.org/uc/item/0vc4s125>

Author

Marumo, Chisato

Publication Date

1976-04-01

REACTIONS AND WETTING BEHAVIOR IN THE
ALUMINUM-FUSED SILICA SYSTEM

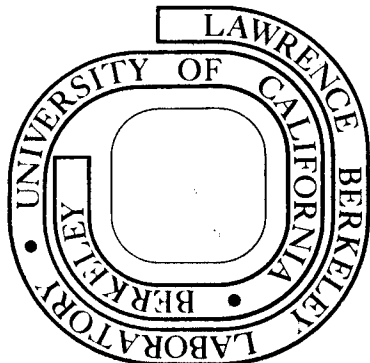
Chisato Marumo and Joseph A. Pask

April 1976

Prepared for the U. S. Energy Research and
Development Administration under Contract W-7405-ENG-48

For Reference

Not to be taken from this room



DISCLAIMER

This document was prepared as an account of work sponsored by the United States Government. While this document is believed to contain correct information, neither the United States Government nor any agency thereof, nor the Regents of the University of California, nor any of their employees, makes any warranty, express or implied, or assumes any legal responsibility for the accuracy, completeness, or usefulness of any information, apparatus, product, or process disclosed, or represents that its use would not infringe privately owned rights. Reference herein to any specific commercial product, process, or service by its trade name, trademark, manufacturer, or otherwise, does not necessarily constitute or imply its endorsement, recommendation, or favoring by the United States Government or any agency thereof, or the Regents of the University of California. The views and opinions of authors expressed herein do not necessarily state or reflect those of the United States Government or any agency thereof or the Regents of the University of California.

REACTIONS AND WETTING BEHAVIOR
IN THE ALUMINUM-FUSED SILICA SYSTEM

Chisato Marumo[†] and Joseph A. Pask
Materials and Molecular Research Division, Lawrence Berkeley Laboratory
and Department of Materials Science and Engineering, University of
California, Berkeley, California 94720

Wetting of fused silica by molten aluminum at temperatures of 800 to 1000°C and 3×10^{-5} torr was dependent on the formation of a reaction zone by redox reactions. The reaction zone consisted of three layers. It was postulated that reactions proceeded by interdiffusion of Si^{++} , Al^+ , Al^{++} and Al^{3+} . The layer adjacent to the metal drop was primarily AlO stabilized by a solid solution of SiO ; and adjacent to fused silica, a spinel of AlO and Al_2O_3 stabilized by SiO . On cooling these dissociated into Al , Si and $\theta\text{-Al}_2\text{O}_3$ and/or $\alpha\text{-Al}_2\text{O}_3$.

1. Introduction

Reactions and wetting behavior in ceramic-metal systems are of technological interest as well as scientific interest in the fields of cermets, composites and electronics. The degree of wetting of a solid by a liquid in a solid-liquid-vapor system has been expressed by Young's equation under chemically stable and metastable equilibrium conditions. Aksay, Hoge and Pask¹ treated the thermodynamics of wetting in a solid-liquid-vapor system by considering the conditions that minimize the total free energy of the system. They also extended their analysis to non-equilibrium conditions. They showed that an interfacial reaction resulted in the lowering of the solid-liquid interfacial tension by a contribution of the free energy of the reaction which could result in the spreading of a liquid drop on a solid substrate.

Reactions between Al and fused SiO_2 are thermodynamically favorable. Standage and Gani² studied the effect of up to 2.5 wt % additions of Bi and Sb on this reaction at 660 to 800°C by dipping fused SiO_2 rods into molten Al and the alloys in air. They detected Si and η -, θ -, and α - Al_2O_3 as reaction products. They proposed that a complex interfacial layer formed by absorbed water and alloying elements with SiO_2 affected the dwell or incubation time of the reaction and the subsequent reaction kinetics. They suggested that at low concentrations of Bi and Sb diffusion was not rate controlling and that at higher concentrations diffusion might be rate controlling. Prabripataloong and Piggott³ studied the same reaction in a similar manner but in vacuum. They observed that the dwell time was drastically reduced under vacuum as compared to air. They suggested that the presence of an Al_2O_3 film on the surface of molten Al in air caused the increased dwell time of the reaction and denied the existence of complex interfacial layers proposed by Standage and Gani.

Prabripataloong and Piggott^{4,5} also studied the reaction between an Al thin film and a fused SiO_2 plate in vacuum. Solid state reactions took place as low as 400°C. The reaction products observed were θ - and α - Al_2O_3 and Si below the melting point of Al. Above the melting point of Al, only Si was detected and they indicated the formation of a volatile oxide of Al.

Yanagida and Kroger⁶ studied the stability of aluminum suboxides in the solid state. They heated Al- Al_2O_3 mixtures in an inert atmosphere and examined the microstructure of the quenched specimens. They indicated that there was no significant change of the melting point of

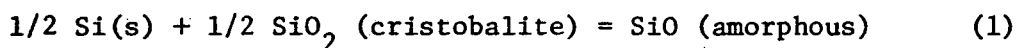
Al_2O_3 by the addition of Al, at least up to 50 wt%. They also concluded that stable solid AlO was not formed.

Low energy electron diffraction (LEED) studies of the (001) surface of $\alpha\text{-Al}_2\text{O}_3$ have indicated a structural transformation upon heating in vacuum.⁷⁻⁹ Charig and Skinner⁷ were the first to suggest that this transformation is due to the formation of an oxygen deficient surface phase with respect to the bulk structure of Al_2O_3 . Based on this observation, Brennan and Pask¹⁰ postulated that at temperatures above 900 to 1000°C and at low pressures an oxygen deficient surface of some unknown thickness exists containing some AlO in a spinel-type structure. They also postulated that on cooling in vacuum this structure persists; however, on exposure to oxygen or moisture the distribution of cations remains essentially the same but the valence of Al^{++} increases to Al^{3+} resulting in a $\gamma\text{-Al}_2\text{O}_3$ type of structure.

Yamaguchi¹¹ studied the oxidation of Al surfaces and presented electron diffraction patterns which provided evidence for the existence of aluminum suboxides between Al and Al_2O_3 on the Al surface oxidized at 300°C.

Stability of solid SiO at high temperatures has been discussed by a number of investigators. Solid SiO has been prepared in a metastable amorphous or poorly crystallized form by condensation of SiO gas upon a cold surface, but it begins to disproportionate to Si and SiO_2 at an appreciable rate around 400-700°C. Gel'd and Kochnev¹³ claimed to have prepared amorphous SiO by heating an intimate mixture of SiO_2 and Si to 1250-1350°C. On the other hand, Schäfer and Hörnle,¹⁴ Grube and Speidel,¹⁵ and Von Wartenbert¹⁶ reported that amorphous SiO is unstable at about 1000-1150°C.

Brewer and Edwards¹² found no evidence of formation of solid SiO by high temperature X-ray diffraction analysis of mixtures of Si and SiO₂ below 900°C, and indicated that solid SiO is thermodynamically unstable and disproportionates to Si and SiO₂ below 900°C. Hoch and Johnston¹⁷ presented evidence for an x-ray pattern of SiO at 1250 to 1350°C, but Geller and Thurmond¹⁸ pointed out that the organic cement used in the samples would form SiC and that the observed x-ray pattern was similar to that expected for a mixture of SiC and β-cristobalite. Potter¹⁹ reported that a mixture of Si and SiO₂ was not liquified at 1700°C, and Brewer and Edwards¹² confirmed a higher melting point for the Si-SiO₂ mixture than for either of its components. Brewer and Greene²⁰ made a differential thermal analysis of a Si-SiO₂ mixture up to the melting point of Si and did not detect any evidence of the formation of stable solid SiO. They postulated that the higher melting point of a Si-SiO₂ mixture formerly reported¹² may have been due to the partial reduction of SiO₂ to SiO_{2-x}. Brewer and Edwards¹² estimated that



$$G^\circ_{298^\circ\text{K}} = 0.0 \pm 3.3 \text{ Kcal}$$

$$G^\circ_{1200^\circ\text{K}} = -0.9 \pm 6.6 \text{ Kcal}$$

The uncertainty is too large to allow any decisive conclusions from the thermodynamic data alone. However, it was noted that there is a definite trend toward increase in stability as temperature is increased. Experimental evidence has been consistent about the existence of metastable amorphous SiO at room temperature which disproportionates on heating, but there is no firm evidence to support the formation of solid SiO by

heating the Si-SiO₂ mixture to high temperatures.

It is significant that no reports have been made of studies of suboxides of Al or Si in the presence of the other. Although AlO is unstable as a bulk phase, it is possible that it is stabilized by forming a solid solution with SiO since its free energy would be reduced by the formation of a solid solution. Tressler, Moore and Crane²¹ studied the reactions between Ti and Al₂O₃. They postulated the possibility of a substantial amount of Al ions in solution in the NaCl-type TiO phase on the basis of a larger unit cell than that for TiO. Also, considering the presence of oxygen-deficient alumina surfaces under low partial pressures of oxygen, it is possible that spinel structures containing Al₂O₃ and AlO, particularly with SiO in solid solution, could form under certain conditions and compositions.

The objectives of this research were to study and understand the reaction mechanisms between fused SiO₂ and molten Al present in a limited amount and the effect of the interfacial reactions on wetting behavior.

2. Experimental procedure

2.1 Materials and Specimen Preparation

The sessile drop technique was used to study wetting behavior and to provide specimens for reaction studies. The Al^{*} was obtained in the form of 1/4 in. diameter rods. Pieces weighing approximately 0.1g were cut from these rods and ground into spheres. Pieces used for x-ray diffraction study weighed approximately 1.0g. The fused SiO₂^{**} used for substrates in the sessile drop experiments was obtained as transparent optically polished plates 1/8 in. or 1/4 in. thick, which were cut into 3/4 in. squares. Both the Al and SiO₂ specimens were cleaned ultrasonically in isopropyl alcohol.

2.2 Experimental Conditions

The sessile-drop furnace has been described previously.¹⁰ The Ta-foil resistance tube was connected to water-cooled copper electrodes by copper holders. The fused SiO₂ plaques rested on the flat surface of an alumina "dee" tube which was fitted inside the Ta-foil tube. The total pressure of the furnace was always kept less than 3×10^{-5} torr during experiments. The temperature was measured with a Pt-Pt 10% Rh thermocouple placed inside the "dee" tube. Contact angle measurements were made over the temperature range of 660-1200°C through fused SiO₂ windows in the vacuum chamber with a telescope to an accuracy of $\pm 1^\circ$.

2.3 Analysis of the Experiments

After cooling, the specimens were cut and polished to examine the interfacial region with an optical microscope and a scanning electron

* United Mineral & Chemical Corp., New York, N.Y. (99.999%)

** Thermal American Fused Quartz Co., Montville, N.J. (>99.97% purity)

microscope. Compositions in the cross-sections perpendicular to the interfaces were determined by an electron microprobe. Line scanning of approximately 75 μm length parallel to an interface was used to obtain an average composition at a given distance from the interface. Spot scanning was also used to analyze regions near boundaries. The reaction phase products were analyzed by X-ray diffraction.

3. Experimental Results

3.1. Sessile Drops of Molten Al on Fused SiO_2

Preliminary experiments at 800°C indicated that the contact angle using spherical pieces of Al changed smoothly, while the contact angle using cubic pieces of Al changed irregularly. The latter were inconsistent because of interfacial reactions prior to the formation of spherical drops on melting of Al. Spherical pieces of Al were thus used to measure advancing contact angles since on melting the periphery of the drop comes in contact with initially unreacted SiO_2 .

The temperature dependence of the contact angle is shown in Fig. 1. The temperature was raised continuously at the rate of 10°C/min from 660°C, the melting point of aluminum, to 1200°C. The dynamic contact angle decreased with temperature with an arrest at 90° in the temperature range of about 900 to 950°C.

Contact angle changes with time at 800 and 900°C are shown in Fig. 2. At 800°C the angle changed continuously until it reached 67° after approximately 50 minutes. The periphery of the Al drop kept in contact with SiO_2 fresh surface up to an angle of 90°; below 90° the periphery was in contact with the reaction zone. During cooling, cracks appeared in SiO_2 near the SiO_2 -reaction zone boundary because of the large

difference in coefficients of thermal expansion. Cross-sections of specimens perpendicular to the Al-SiO₂ interface after 17 min. are shown in Fig. 3(a) and after 40 min., in Fig. 3(b). The microstructure of the metal drop in the former shows Al and an eutectic mixture; and in the latter, Si and an eutectic mixture. The eutectic temperature is 577°C and composition, 12.6 wt. % Si. The 40 min. specimen also shows a higher concentration of Si near the interface and near the surface of the drop.

At 900°C, the growth rate of the reaction layer was always faster than the flow rate of molten Al so that the periphery of the drop was always in contact with the reaction zone. The reduction of the contact angle to about 80° occurred in about 10 min. The continued reduction of the contact angle was slow, taking about 3 hours to reach 70°.

3.2 Reactions between Molten Al and Fused SiO₂

Reaction studies were based on examination of sessile drop configurations of Al on fused SiO₂ heated at 800, 900 and 1000°C for 60 minutes; and of Al with 28.3 wt % Si (which corresponds to saturation with Si at 800°C) on fused SiO₂ heated at 800°C for 24 hours.

Reactions always occurred at the liquid-solid interfaces with a replacement of Al in the drop with Si as described above, and of Si in the substrate with Al. The liquid-solid interfaces did not move, but the interfaces between the reaction zone and unreacted SiO₂ moved. The reaction zone consisted of three layers which were classified as: I (adjoining the drop), II, and III (adjoining the unreacted SiO₂). The notation a in subsequent references indicates 900°C; b, 800°C; c, Al-Si alloy at 800°C; and d, 1000°C. The optical micrograph of the cross-

section of the specimen perpendicular to the interface after reacting at 1000°C for 1 hour is shown in Fig. 4.

The composition of the reaction layers was analyzed with an electron microprobe. The percent atomic compositions, after being corrected by computer^{*}, are shown for 800°C in Fig. 5 and for 1000°C in Fig. 6(a) after one hour reaction times. Figure 4 shows the paths along which composition analyses were made for the 1000°C specimen. No concentration gradients were detected in the matrix of layer I which always had a fine homogeneous structure. Concentration gradients were present in layer III-d at 1000°C which also had a fine homogeneous structure, and probably in III-b at 800°C. Analysis of layer II indicated irregularities suggesting the presence of several phases at temperature. Compositions of coarser-grained areas in Layer I adjacent to the drop interface were similar to those of Layer II. Atomic percentage compositions of a number of reaction layers are given in Table I. In all cases, Al and Si were measured directly and the oxygen was determined by difference.[†]

The thicknesses of the reaction layers within the reaction zone are dependent on temperature and composition of the liquid drop. With Al, the dominant layer at 800°C is I-b. For 1 hour reaction times, it decreases in thickness at 900°C and again at 1000°C. Layers II-b and III-b, on the other hand, are too thin for accurate analysis at 800°C,

* Corrections were made for deadtime losses, background absorption, characteristic fluorescence, back scatter losses, and ionization penetration losses.

† The profiles shown in Fig. 4 were also measured directly for Al, Si and oxygen by JEOL USA, Inc., Medford, Massachusetts; the normalized profiles within experimental error were similar to those in Fig. 6(a).

but increase in thickness with temperature. The overall thickness of the reaction zone, however, was essentially the same after one hour of reaction at 800, 900 and 1000°C. Figure 7 is an optical micrograph of a cross-section of a specimen held at 1000°C showing Layers I-d, II-d, III-d and SiO₂ at the bottom. Figure 8 shows x-ray fluorescence micrographs for Al-K α and Si-K α of a specimen heated at 900°C indicating Layers I-a, II-a and III-a (bottom); it can be seen that the Si content in II-a is higher than in I-a and III-a and that its distribution is more irregular. With Al-28.3 wt % SiO₂ at 800°C the layers were II-c and III-c, and Layer I-c did not form; an approximately equivalent thickness of overall reaction zone was obtained after 20 hours. Figure 9 shows x-ray fluorescence micrographs of a cross-section of a specimen showing Layers II-c, III-c and SiO₂ (bottom).

Reaction products present at room temperature in layers thick enough to be analyzed were determined by x-ray diffraction. Layers I-b and I-a after one hour of reaction were composed of θ -Al₂O₃, α -Al₂O₃, Al and Si. Layers II-a and II-d showed α -Al₂O₃, Al and Si. Layer III-d showed θ -Al₂O₃, Al and Si.

4. Discussion

4.1. Wetting Behavior

The contact angle of a steady state sessile drop in a solid-liquid-vapor system in the absence of a chemical reaction is determined by the relative magnitudes of the three interfacial tensions. Yin²² showed that the rate of increase of the solid-liquid interfacial area as the system approaches this static or steady state equilibrium condition is linear and only a function of viscosity, surface tension, and initial

contact angle. If there is a reaction at the solid-liquid interface, however, the reduction of γ_{sl} due to the contribution of the free energy of the reaction $(-)\Delta g^{sl}$ must be considered.¹

Since the Al becomes enriched in Si during the reaction, the change of its γ_{lv} and viscosity η has to be taken into account. The surface tension of Al at 800°C is 860 dyne/cm and at 900°C 850 dyn/cm.²³ The extrapolated value of the surface tension of Al to 1450°C is 810 dyne/cm. The surface tension of Si (m.p. 1410°C) at 1450°C is 730 dyne/cm.²⁴ The component which has a lower surface tension is present at a higher concentration in the surface compared to the bulk ideal mixture in a binary liquid. As shown in Fig. 3(b), the Si concentration at the surface of the drop is higher, indicating that the dissolution of Si lowers the surface tension of the aluminum liquid. The viscosity η for pure Al is 1 cP and that for Al-28 wt% Si is 0.8 cP at 800°C.²⁵ Consequently, the viscosity of Al itself and its change with Si solution is so small that its effect on wetting can be considered to be negligible. Therefore, the first decrease of contact angle is considered to be mainly due to the contribution of the free energy of the reaction $(-)\Delta g^{sl}$ and subsequently also to the decrease of the surface tension of the liquid.

If there was no reaction, the contact angle would be obtuse since γ_{sv} of fused SiO_2 is ~300 dyne/cm which is smaller than γ_{lv} . The contact angle, however, decreased because of the contribution of the free energy of the reaction to the reduction of the interfacial energy γ_{sl} . At 800°C the periphery of the drop kept in contact with the unreacted SiO_2 surface down to ~90°. Below this angle, because of a reduction in the driving force for the reaction due to the increase of the Si

concentration in the liquid and because of the energy necessary for extension of the liquid surface, the growth rate of the reaction zone exceeded the flow rate of the liquid. Below a contact angle of $\sim 90^\circ$, the periphery of the drop thus remained in contact with Layer I. At 900°C , the growth rate of the reaction zone was always faster than the flow rate of molten Al, and the reaction proceeded through the reaction zone. The contact angle dropped rapidly below 90° , and the periphery of the drop remained in contact with Layer II.

The difference in the wetting behavior at 800°C and at 900°C (Fig. 2) is due primarily to the faster rate of the reaction at the higher temperature and to the difference of the nature of the reaction. This transition of the wetting behavior is reflected in the change of the slope of the temperature dependence of the contact angle and the arrest at $\sim 900^\circ\text{C}$ (Fig. 1).

4.2. Nature of Reactions

Room temperature phase analysis by x-ray diffraction indicates α - and/or θ - Al_2O_3 , and Al and Si in all three layers. If Al^{3+} , Al° and Si° were actually the species that existed at the reaction temperatures, it would be necessary to have the redox (oxidation-reduction) reaction occur at the SiO_2 interface to form a replacing Al_2O_3 matrix through which Al° and Si° interdiffuse. In addition, with no loss of oxygen, the Al_2O_3 content throughout the reaction zone would have to remain constant. There would not then be any logical explanation for the existence of the three reaction layers with the indicated concentration profiles. Any possible reaction mechanism based on penetration of molten Al into the reaction zone thus has to be discarded.

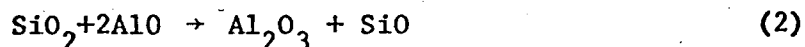
It is postulated that ionic interdiffusion occurs at the reaction temperatures and that the diffusing ionic species in the reaction zones are Si^{++} , Al^+ , Al^{++} and Al^{3+} because of the presence of Al and a constant O^{2-} content or no oxygen transport. On cooling, AlO and Al_2O dissociate to Al and Al_2O_3 ; in the presence of SiO , the dissociation reaction products are Al, Si, and Al_2O_3 . Since this dissociation involves short range diffusion as indicated by the microscopic homogeneity of layers I and III, the atomic concentration profiles are not affected.

On the basis of this postulate, it is possible to make a normative type of analysis using atomic percentage profiles, such as shown in Figs. 5 and 6(a), to calculate percentage profiles for the various ionic species expected at the test temperatures. Because of the high oxidation potential of Al it is expected that Si^{4+} in the fused SiO_2 is reduced to Si^{++} which is present throughout the reaction zone. Each Si^{++} requires one O^{2-} for charge balance. The amount of the remaining oxygen ions determines the amount and distribution of Al^+ and Al^{++} , or Al^{++} and Al^{3+} . On this basis an atomic percent of oxygen of 50% indicates the presence of Al^{++} with the Si^{++} ; less than 50%, of Al^+ and Al^{++} ; and more than 50%, of Al^{++} and Al^{3+} . Table I shows average atomic percent and calculated average ionic percent compositions for several reaction layers. Since the Al-Layer I interface has not moved, it can be assumed that the oxygen content remains constant throughout the reaction zone. Ionic concentration profiles can then be calculated on this basis; the ionic percentage data for 1000°C in Table I is thus recalculated to give the numbers of cations per 66 oxygens which correspond to the atomic or ionic number in SiO_2 , and are plotted as Fig. 6(b). Reaction mechanisms

can now be postulated.

1. Layer III

At the SiO_2 interface a redox reaction occurs with the movement of the interface into the SiO_2 according to



in which Si^{4+} is reduced to Si^{++} , and Al^{++} is oxidized to Al^{3+} to form Layer III. The reaction, as indicated in the profile of Fig. 6(b), is thus dependent on chemical interdiffusion of Al^{++} and Si^{++} in the product layer. It is expected that this interdiffusion is the slow step and controls the growth of the layer which becomes appreciable at $\sim 900^\circ\text{C}$ and increases with temperature. The lack of a gradient in the Al^{3+} profile and lack of solution of Al_2O_3 in SiO_2 indicates extremely slow interdiffusion of Al^{3+} and Si^{4+} at all of these test temperatures and essentially equilibrium compositions at this interface.

The nature of the structure of this layer at temperature can be deduced for a specimen heated at 1000°C for 1 hour, by calculating the molar compositions from data in Fig. 6(b) and Table II. As an example, a composition of 39 at% Al, 4 at% Si and 57 at% O becomes $(0.29\text{SiO} \cdot 0.78\text{AlO})1.00\text{Al}_2\text{O}_3$ which represents essentially stoichiometric spinel. Calculated compositions are very sensitive to the accuracy of the electron microprobe measurements: a 1 at% decrease in Al with a corresponding increase in O results in a large excess of Al_2O_3 over the stoichiometric, and a 1 at% increase in Al results in a large decrease of Al_2O_3 . Even though AlO and probably SiO by themselves are unstable, it is postulated that stability exists under the conditions of the

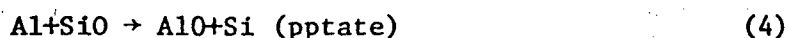
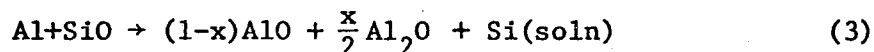
experiment in a spinel structure with Al_2O_3 . On cooling, the previously indicated decomposition occurs to form Al, Si and $\theta\text{-Al}_2\text{O}_3$ which has a monoclinic cell and a structure that can be described as a deformed spinel type.

2. Layer I

The reaction at the droplet interface and the growth of Layer I are more complicated. It is significant that these layers did not show any concentration gradients, that the layer thickness decreased with increase of temperature, and that the layer did not form when the starting Al was saturated with Si in experiments at 800°C . Comparing the compositions of Layer I at 800, 900, and 1000°C (Tables I and II), it can be seen that with the indicated scatter of microprobe values, as represented in Fig. 5, the atomic compositions are essentially AlO and some SiO although there is a trend toward a small increase of oxygen with temperature. The molar composition is very sensitive to these small variations in the atomic composition: for the average values given in the tables, 49 at% of O at 800°C results in 4.1 mole % of Al_2O and 51 at% of O at 1000°C results in 4.3 mole % of Al_2O_3 --the balance of the mass in both cases being SiO and AlO. It is likely, however, that the small amount of calculated Al_2O_3 does not exist in this layer and is due to the indicated experimental scatter. In any case, a given molar composition is expected to be present as a solid solution which provides its stability at temperature.

When the starting Al drop is not saturated with Si, the redox reaction at the interface (Eq. 3) causes the reduced Si to go into solution in the molten Al (the degree of Si solution determines the amount

of precipitates of Al or Si that form on cooling, Fig. 3). When the Al drop is saturated with Si, the redox reaction (Eq. 4) results in precipitation of Si in the drop at test temperature.



This analysis suggests that when Al is not saturated with Si, oxidation of Al results in the formation of some Al^+ in addition to Al^{++} . When Al is saturated with Si, it appears that Al^+ does not form and possibly some Al^{3+} may form.

The Al^+ reacts with Al^{3+} , which forms at the SiO_2 -Layer III interface and is part of Layers III and II, at the Layer II-Layer I interface to form Al^{+2} (Eq. 5) which is the major constituent of Layer I, resulting in its growth.



In the absence of Al^+ , this reaction does not occur and no growth of Layer I occurs. Thus, Layer I grows until the Al becomes saturated with Si; at that point Layers III and II grow at the expense of Layer I which now has no Al^+ . Another factor contributing to this general pattern of layer formation is an expected larger increase of \tilde{D} with temperature in Layer III than in Layer I. The summation of these effects plus the limited amount of available Al in the drop must result in the observed essentially constant reaction zone with temperature.

In any case the driving force for interdiffusion of cations in a layer of constant composition is the electrochemical potential gradient initiated by the presence of unoxidized Al in the drop. The nature of

the structure at temperature can be deduced by calculating the molar composition from data in Table II which is essentially AlO with some SiO and some Al₂O in solid solution. It is postulated that solid AlO is stabilized by this solution. On cooling to room temperature it decomposes to form α- and θ-Al₂O₃, Al and Si.

3. Layer II

Layer II, on the basis of its microstructure, is considered to have been a multi-phase region at test temperature consisting of AlO, SiO and Al₂O₃ solid solutions with precipitates of α-Al₂O₃ whose formation is considered to be due to an excess of Al³⁺ from Layer III and a limited amount of Al⁺ from Layer I. In a three-component diffusion couple, an intermediate two phase region can be expected. The precipitates in the matrix do not disturb the diffusion paths. At room temperature, the phases are Al, Si and α-Al₂O₃. On dissociation during cooling the α-Al₂O₃ precipitates can provide nucleation sites for continued α-Al₂O₃ growth which can be enhanced by the release of oxygen by the dissociation of a larger amount of SiO in Layer II in comparison with I and III.

In conclusion, the thickness of each reaction layer is determined by its relative growth rate under the existing conditions. At 800°C, Layer I grows when Al is not saturated with Si but does not form when Al is saturated with Si due to the formation of some Al⁺ in the former case in addition to Al⁺⁺. Layers II and III form slowly and are too thin for analysis after one hour. At 900 and 1000°C, growth of Layers II and III is accelerated because of increased \tilde{D} through Layer II and because the growth of Layer I stops when Al becomes saturated with Si by reaction at which point Layer II grows at its expense.

0 0 0 0 0 0 0 0 0 0 0 0

ACKNOWLEDGMENT

The authors wish to express their thanks to George Georgakopoulos and Richard Lindberg for their assistance with the electron microprobe and the electron scanning microscope. Thanks are also extended to Mr. F. Jimbo of JEOL USA, Inc., who arranged for the electron microprobe analysis of one of the specimens.

The financial support for the research by Kanebo, Ltd., Osaka, Japan, and the Energy Research and Development Administration is acknowledged.

References

1. I. A. AKSAY, C. E. HOGE, and J. A. PASK, J. Phys. Chem., 78 (12), (1974) 1178.
2. A. E. STANDAGE and M. S. GANI, J. Am. Ceram. Soc., 50 (2), (1967) 101.
3. K. PRABRIPUTALOONG and M. R. PIGGOTT, J. Am. Ceram. Soc., 56 (4), (1973) 184.
4. K. PRABRIPUTALOONG and M. R. PIGGOTT, J. Am. Ceram. Soc., 56 (4), (1973) 177.
5. K. PRABRIPUTALOONG and M. R. PIGGOTT, J. Electrochem. Soc.: Solid State Science and Technology, 121 (3), (1974) 430.
6. H. YANGIDA and F. A. KRÖGER, J. Am. Ceram. Soc., 51 (12), (1968) 700.
7. J. M. CHARIG and D. K. SKINNER, "Proceedings of the Conference on the Structure and Chemistry of Solid Surface", G. A. Somorjai, ed., John Wiley and Sons, New York, (1969) p. 34.
8. C. C. CHANG, *ibid.*, p. 77.
9. T. M. FRENCH and G. A. SOMORJAI, J. Phys. Chem., 74 (12), (1970) 2489.
10. J. J. BRENNAN and J. A. PASK, J. Am. Ceram. Soc., 51 (10), (1968) 569.
11. S. YAMAGUCHI, Werkstoffe und Korrosion, 25 (5), (1974) 325.
12. L. BREWER and R. K. EDWARDS, J. Phys. Chem., 58, (1954) 351.
13. P. V. GEL'd and M. I. KOCHNEV, Zhur. Priklad Khim., 21, (1948) 1249.
14. H. SCHÄFER and R. HÖRNLE, Z. Anorg. Allg. Chem., 263, (1950) 261.
15. G. GRUBE and H. SPEIDEL, Z. Electrochem., 53 339, (1949) 341.
16. H. von WARTENBERG, Z. Electrochem., 53, (1949) 343.
17. M. HOCH and H. L. JOHNSON, J. Am. Chem. Soc., 75 (1953) 5224.
18. S. GELLER and C. D. THURMOND, J. Am. Chem. Soc., 77, (1955) 5285.

7 4 7 8 0 8 7 0 0 0 0

19. H. N. POTTER, Trans. Am. Electrochem. Soc., 12, (1907) 191, 215, 223.
20. L. BREWER and F. T. GREENE, J. Phys. Chem. Solid, 2, (1957) 286.
21. R. E. TRESSLER, T. L. MOORE, and R. L. CRANE, J. Mater. Sci., 8, (1973) 151.
22. T. P. YIN, J. Phys. Chem., 73 (7), (1969) 2413.
23. S. H. OVERBURY, P. A. BERTRAND, and G. A. SOMORJAI, "The Surface Composition of Binary Systems. Prediction of Surface Phase Diagrams of Solid Solutions", Chem. Rev., to be published.
24. M. HUMENIK, JR. and W. D. KINGERY, J. Am. Ceram. Soc., 37 (1), (1954) 18.
25. V. M. GLAZOV and A. A. VERTMAN, "Structure and Properties of Liquid Metals", A. M. Samarin, ed., Moscow, Academy of Science, U.S.S.R., Baikov's Institute of Metallurgy, 1960, p. 121.

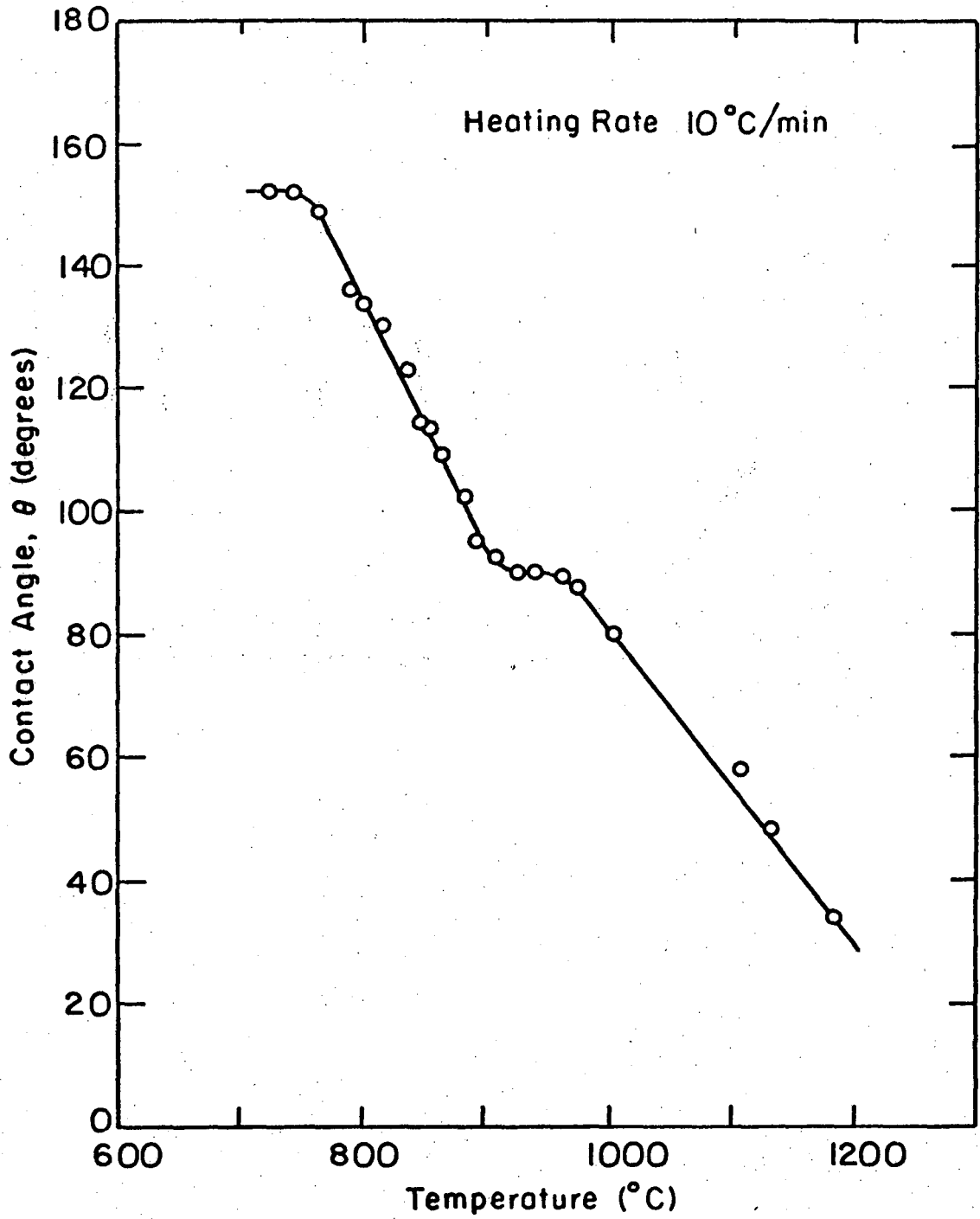
Table I. Average Compositions of Several Reaction Layers after One Hour at Temperature

<u>Layer</u>	<u>Temp.</u>	<u>Atomic Percent</u>			<u>Ionic Percent</u>				
		<u>Al</u>	<u>Si</u>	<u>O</u>	<u>Al⁺</u>	<u>Al⁺⁺</u>	<u>Al³⁺</u>	<u>Si⁺⁺</u>	<u>O²⁻</u>
I-b	800	47	4	49	4	43	-	4	49
I-a	900	46	4	50	-	46	-	4	50
I-d	1000	45	4	51	-	41	4	4	51
II-d	1000	34	13	53	-	22	12	13	53
III-d(Al)	1000	41	4	55	-	21	20	4	55
III-d(SiO ₂)	1000	37	8	55	-	17	20	8	55

00004308475

Figure Captions

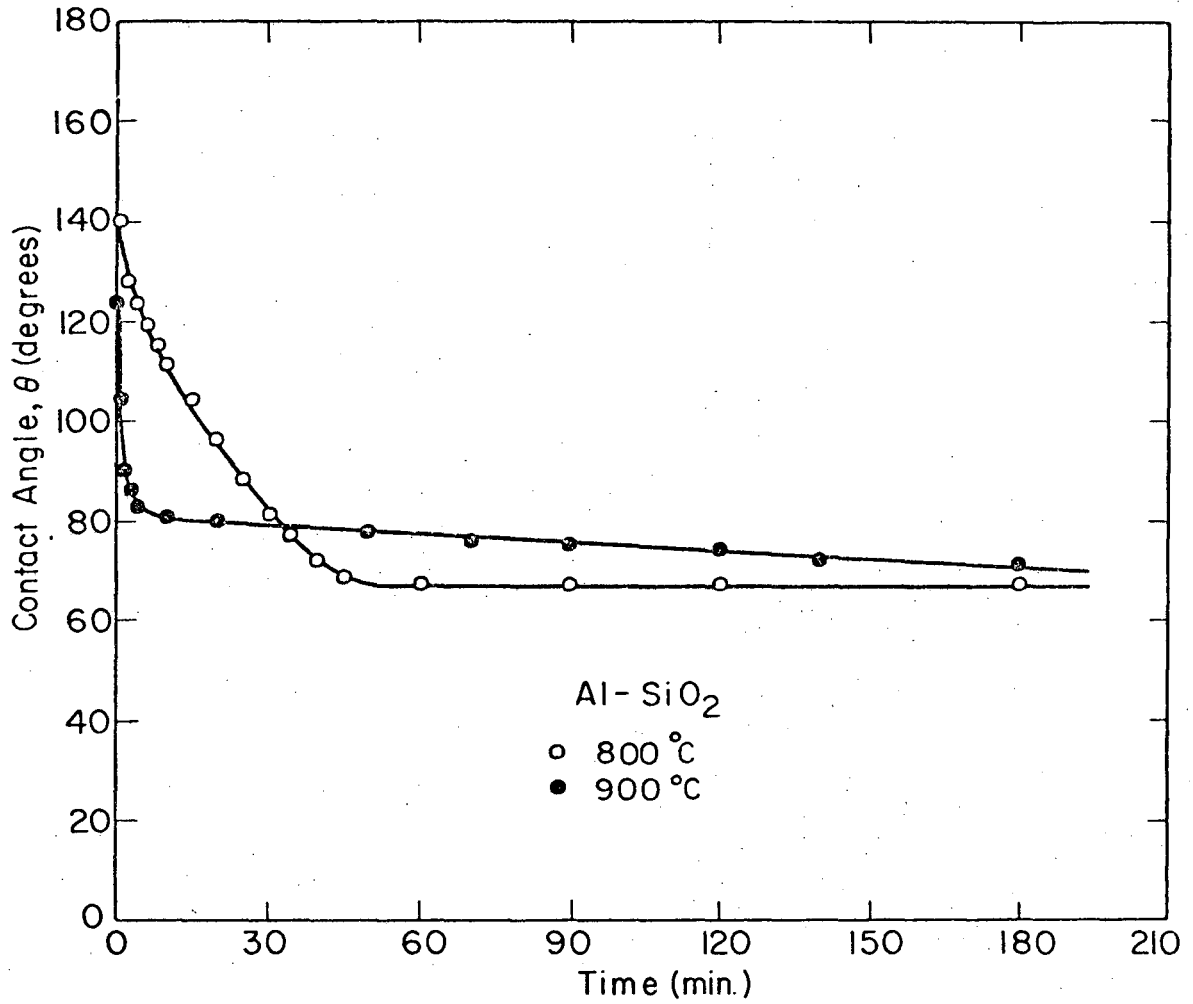
- Fig. 1. Change in advancing contact angle with temperature.
- Fig. 2. Change in advancing contact angle with time at 800 and 900°C.
- Fig. 3. Optical micrographs of Al drop after reaction with SiO_2 at 800°C: (left) for 17 min, Al grains interspersed with Al-Si eutectic; (right) for 40 min, Si grains interspersed with Al-Si eutectic.
- Fig. 4. Optical micrograph of cross-section of an Al-fused SiO_2 specimen after reacting at 1000°C for 1 h.
- Fig. 5. Electron microprobe analysis in at% of a cross-section of an Al- SiO_2 specimen after reacting at 800°C for 1 h.
- Fig. 6. (a) Electron microprobe analysis in at% of a cross-section of an Al- SiO_2 specimen after reacting at 1000°C for 1 h.
(b) Calculated ionic species profiles based on a constant number of oxygen ions using at% concentration data in (a).
- Fig. 7. Enlargement of the areas along the two microprobe paths shown in Fig. 4 indicating layers I-d (top), II-d, III-d, and SiO_2 (bottom).
- Fig. 8. X-ray fluorescence micrographs of the cross-section of a specimen after reacting at 900°C for 1 h. showing layers I-a (top), II-a, and III-a: (top) Al-K α , (bottom) Si-K α .
- Fig. 9. X-ray fluorescence micrographs of the cross-section of a Si-saturated Al (Al-28.3 wt% Si) - SiO_2 specimen after reacting at 800°C for 24 h. showing layers II-c (top), III-c, and SiO_2 : (top) Al-K α , (bottom) Si-K α .



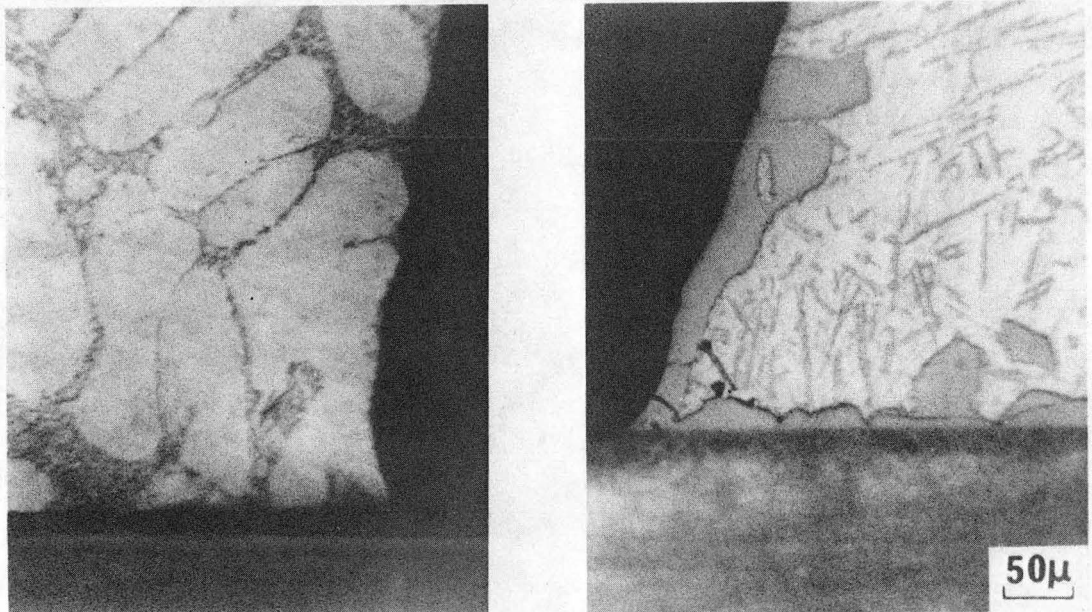
XBL 757-6770

Fig. 1

0 0 0 0 4 3 0 8 4 7 6



XBL 757- 6771A
Fig. 2



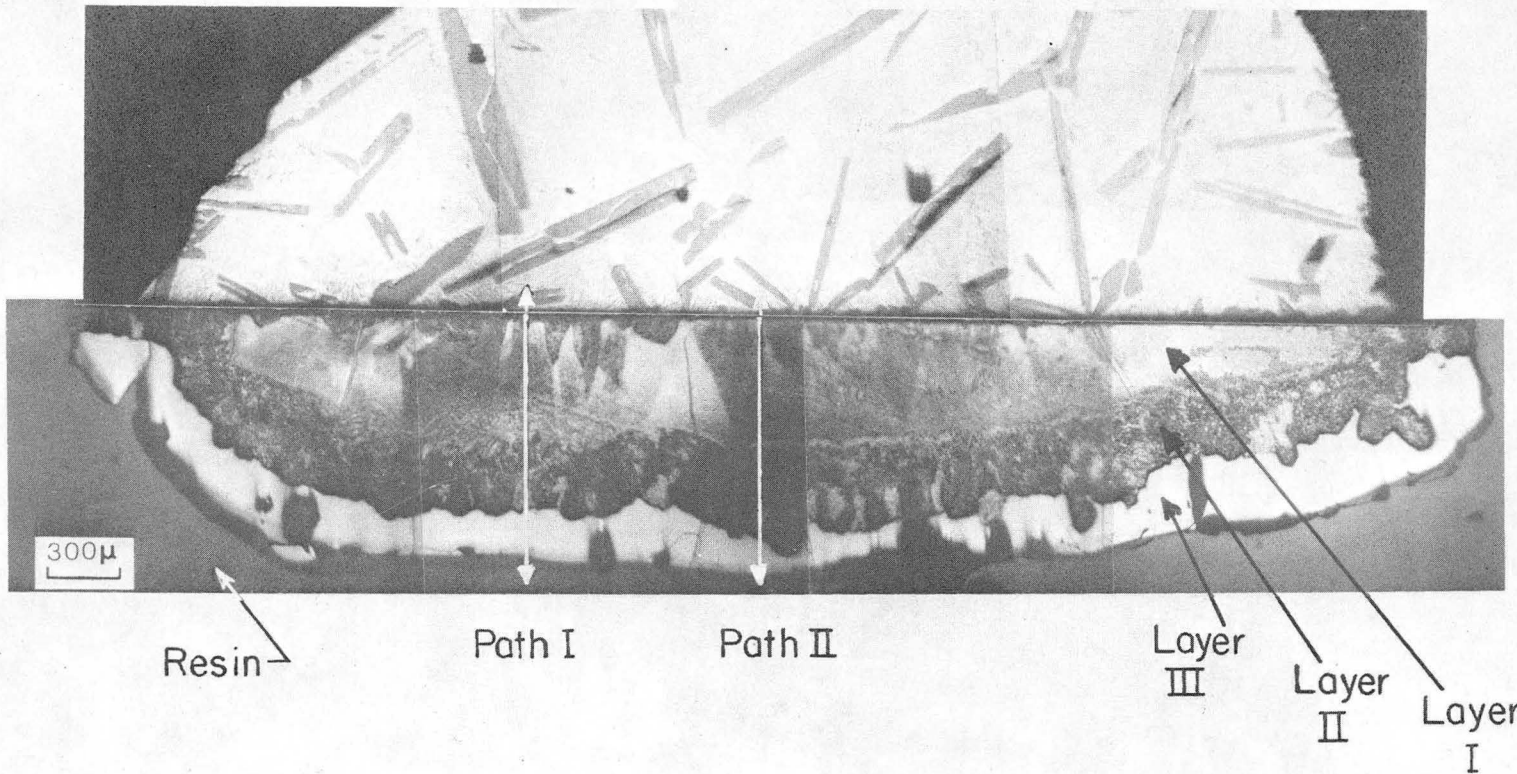
XBB 757-5711A

Fig. 3

00004308477

Al - SiO₂, 1000 °C 1 HR

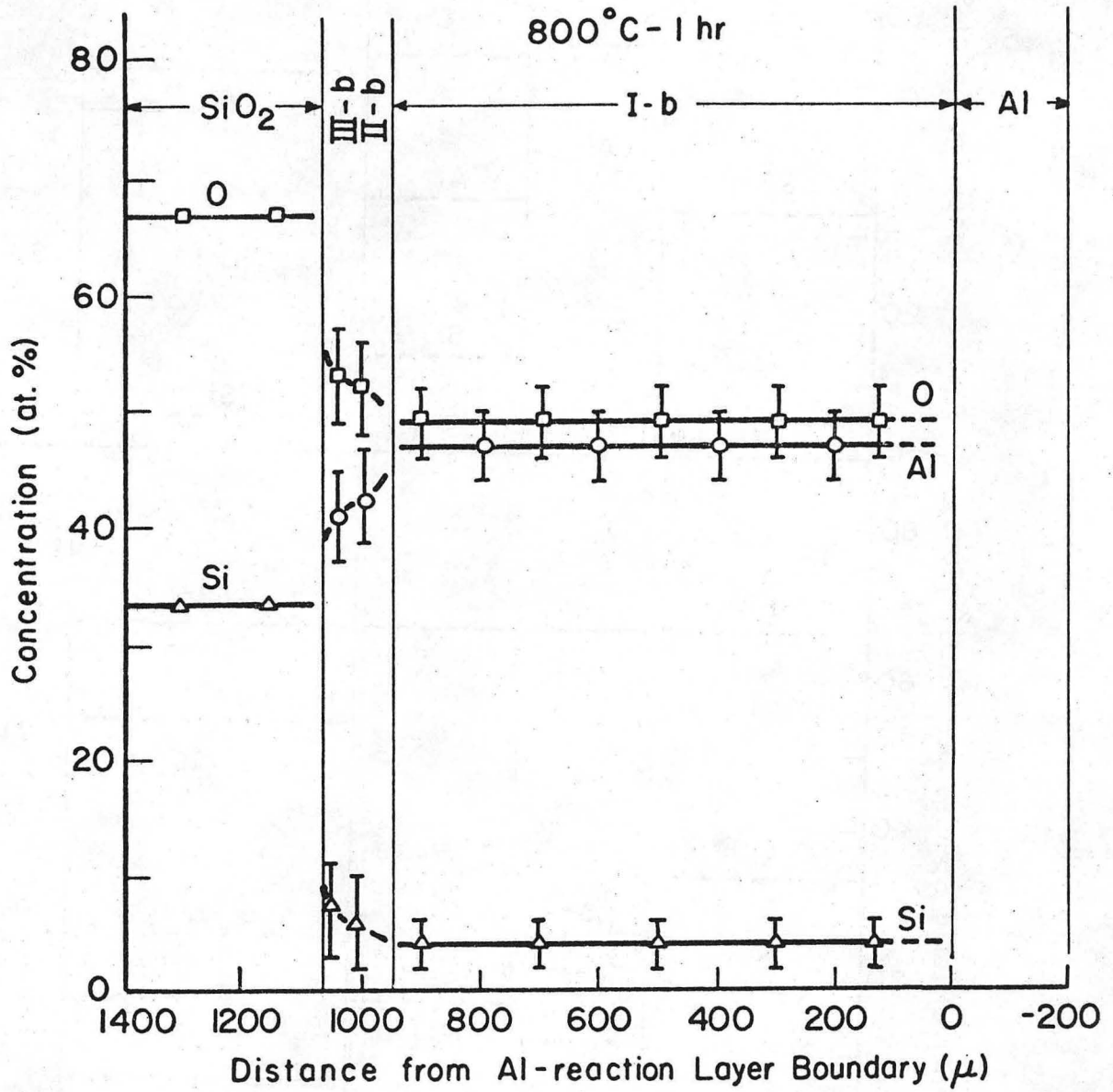
Al drop with Si precipitates



-26-

XBB 759-6822

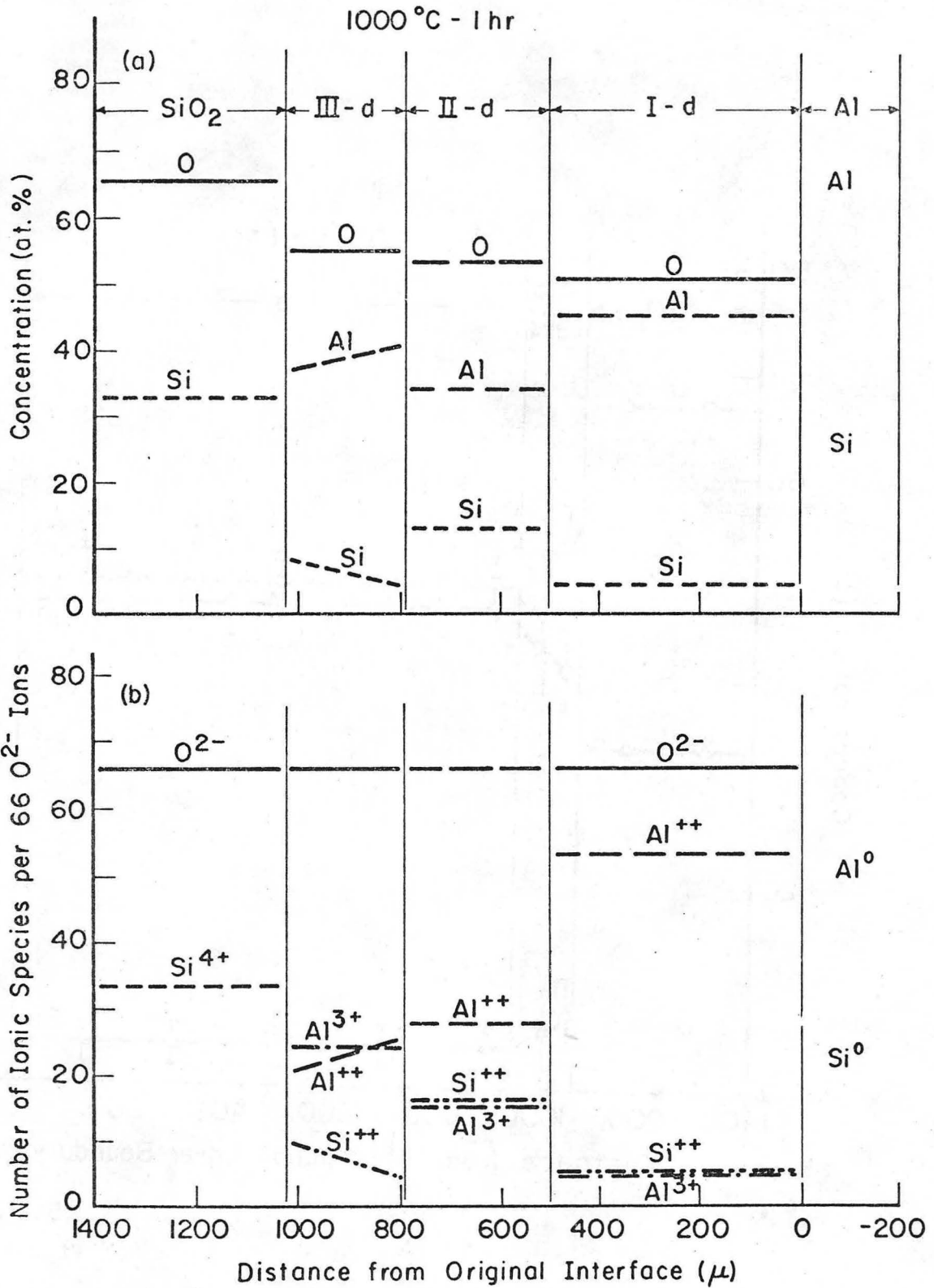
Fig. 4



XBL 764-6657

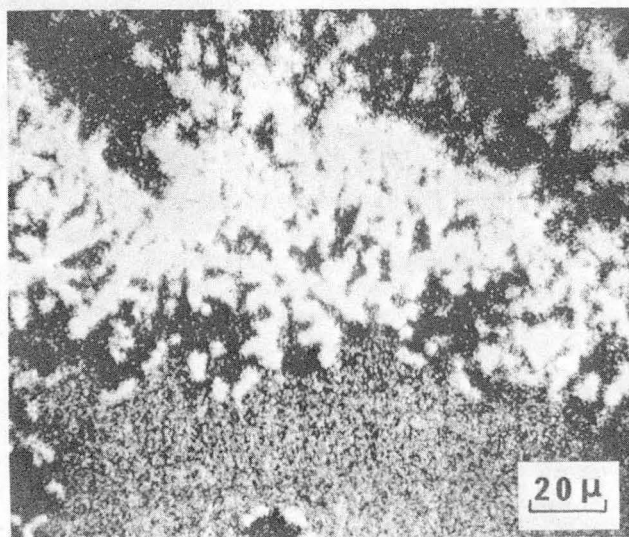
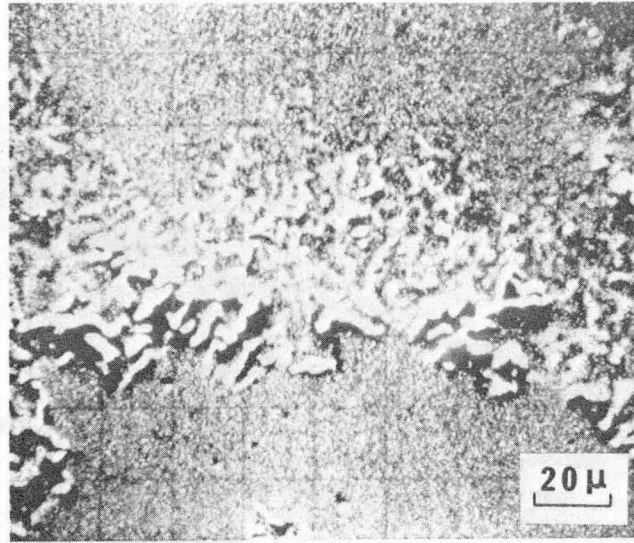
Fig. 5

0 0 0 0 4 3 0 8 4 7 8



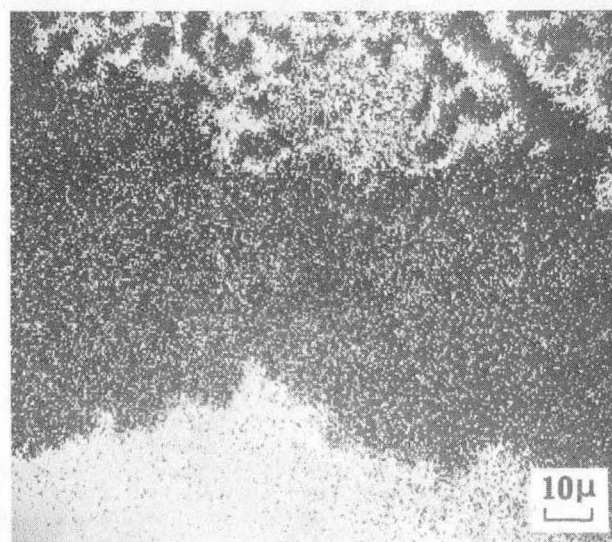
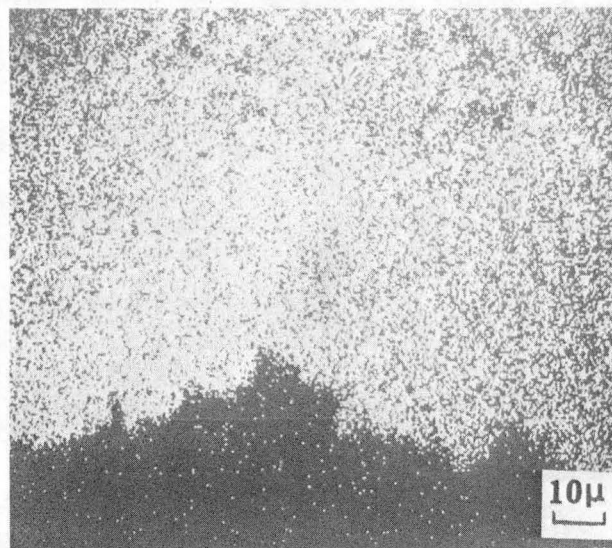
XBL 764-6658

Fig. 6



XBB 757-5707

Fig. 8



XBB 757-5706

Fig. 9

0 0 0 0 4 3 0 8 4 8 0

LEGAL NOTICE

This report was prepared as an account of work sponsored by the United States Government. Neither the United States nor the United States Energy Research and Development Administration, nor any of their employees, nor any of their contractors, subcontractors, or their employees, makes any warranty, express or implied, or assumes any legal liability or responsibility for the accuracy, completeness or usefulness of any information, apparatus, product or process disclosed, or represents that its use would not infringe privately owned rights.

TECHNICAL INFORMATION DIVISION
LAWRENCE BERKELEY LABORATORY
UNIVERSITY OF CALIFORNIA
BERKELEY, CALIFORNIA 94720